VILNIUS TECH
Vilnius Gediminas Technical University

AVIATION
ISSN: 1648-7788 / eISSN: 1822-4180
2022 Volume 26 Issue 1: 1–10
https://doi.org/10.3846/aviation.2022.16589

AIRCRAFT POSITIONING USING MULTIPLE DISTANCE MEASUREMENTS AND SPLINE PREDICTION

Ivan OSTROUMOV[1,*], Karen MARAIS[2], Nataliia KUZMENKO[3]

[1, 3]*Air Navigation Systems Department, National Aviation University, Kyiv, Ukraine*
[2]*School of Aeronautics and Astronautics, Purdue University, West Lafayette, USA*

Received 6 February 2021; accepted 15 June 2021

Abstract. During the crucial phases of take-off, initial climb, approach, and landing where aircraft are close to the ground, Global Navigation Satellite Systems (GNSS) signal strength may not be sufficient to guarantee safe operation, especially in the presence of potential interference, malicious or otherwise, from ground equipment. When the GNSS location is lost, aircraft typically revert to other navigation aids. The most accurate navigation aid is Distance Measuring Equipment (DME). However, whereas GNSS location is triangulated, the navigation equipment on-board aircraft can only measure two DME signals simultaneously. Therefore, location based on DME tends to be accurate only to hundreds of meters, compared to meters for GNSS. A new approach is presented for positioning using multiple DMEs. The approach is based on regression analysis for prediction of DMEs distances in time of measurement. This approach increases positioning accuracy due to availability of multiple DMEs data in the system of navigation equations. Spline functions were used in a regression model in order to achieve the most accurate prediction values. An approach was verified using real flight data and shown the decreasing of navigation system error on value depending on availability and geometry of ground stations locations.

Keywords: DME/DME, APNT, spline, regression, airplane, positioning, navigation, extrapolation, multiple distances.

Introduction

One of the primary roles of air traffic control systems is to keep aircraft safely separated in controlled airspaces. In case aircraft do violate minimum separation standards, backup systems on board aircraft alert crews and suggest escape maneuvers. For any of these systems to work, the positions of all the aircraft in the controlled airspace must be known.

In the past, aircraft position has been primarily determined using ground-based radar systems. When the Global Positioning System (GPS) signal was made available for civilian use in the 1980s, civil aviation started using it as an additional source of location data. Global Navigation Satellite Systems (GNSS), such as the US GPS, European GALILEO, and Russian GLONASS, offer high accuracy, availability, continuity and integrity in comparison with other currently available aircraft positioning systems (International Civil Aviation Organization, 2017). Unfortunately, these systems are also vulnerable to intentional or unintentional jamming, which can degrade accuracy to below safe levels, or even make systems completely unavailable. Further, during the crucial phases of takeoff, initial climb, approach, and landing where aircraft are close to the ground, GNSS signal strength may not be sufficient to guarantee safe operation, especially in the presence of potential interference, malicious or otherwise, from ground equipment (Lubbers et al., 2015).

The number of GNSS failures in the USA has been increasing over time, as shown in Figure 1. From January 2005 to December 2020, there were at least 347 cases of GNSS failures, 250 of which were due to GNSS malfunction, and 97 of which were due to interference or jamming of GNSS signals (NASA, 2020). The number of incidents increased rapidly from 2014–2019, likely due to the increase of air traffic and rapid spread of jamming equipment. For example, in September 2017, the GPS signal around Cairo International Airport was jammed (Federal Aviation Administration, 2017). The Egyptian aviation authority sent alerts to airlines that the GPS was being jammed, and requested that they use alternative positioning equipment to continue operation within RNP/RNAV requirements.

*Corresponding author. E-mail: *ostroumovv@ukr.net*

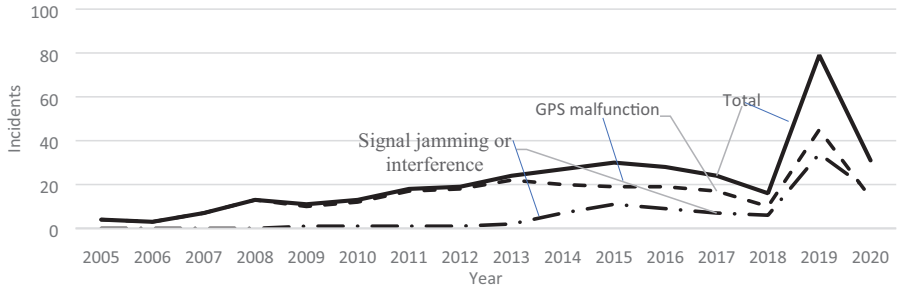

Figure 1. Incidents caused by GNSS malfunction, signal jamming, and interference

Several different options are available in case aircraft location cannot be determined using GNSS. These options are collectively referred to as Alternative Positioning Navigation and Timing (APNT). APNT methods use signals from navigational aids such as Distance Measuring Equipment (DME), Tactical Air Navigation (TACAN), Very High Frequency Omnidirectional Range (VOR), and Non-Directional Beacon (NDB) for positioning (Han et al., 2016; Kim et al., 2019). The most accurate and most promising approach uses DME (Lilley & Erikson, 2012; Lo et al., 2013).

The theoretical accuracy of DME-based approaches to APNT increases as more DME beacons are used. Unfortunately, the on-board DME interrogation system can interrogate at most two beacons at any one time. To overcome this limitation, a novel approach is proposed based on selecting the best combination of position estimates from current DME measurements and predicted positions based on previous DME measurements.

1. DME/DME positioning algorithm

Standard APNT using DME works as follows and as shown in Figure 2. An aircraft determines its slant range to a particular DME beacon by transmitting a Ultra High Frequency (UHF) signal to it and measuring the return delay. Transport category airplanes are equipped with two DME interrogators that can simultaneously interrogate two DMEs. These interrogators are controlled automatically by the Flight Management System (FMS) based on the preplanned flight trajectory via the radio management panel. The FMS internal memory also contains a database that specifies the basic characteristics of the DME beacons (e.g., identification code, operating frequencies, type, and location). When alternative positioning is used, the FMS detects the optimal pair of DME/DME beacons that minimizes the position error and automatically tunes the on-board interrogators to the applicable frequencies (Ostroumov et al., 2018). With two beacons, the aircraft can determine its horizontal position, but not altitude.

When the internal angle α between the two beacons is between 30° and 150°, the Navigation System Error (NSE) is sufficiently small to meet RNAV 1 requirements (International Civil Aviation Organization, 2020). In such cases, ICAO permits using DME/DME positioning as an alternative to GNSS (International Civil Aviation Organization, 2013). Currently, DME/DME is the only approved alternative (Berz, 2008). FMS controls a performance of positioning by DME/DME pair (Ostroumov & Kuzmenko, 2018).

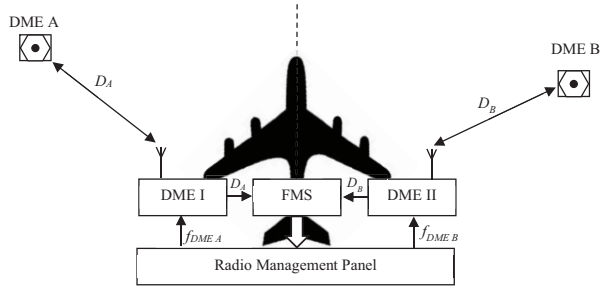

Figure 2. Distance measuring equipment operation

The accuracy of DME-based position determination increases as the number of beacons increases (Kuzmenko et al., 2018). When the geometry is favorable, using all the available DME beacons can in theory result in accuracy comparable to RNAV 1 and better (Vitan et al., 2015; Ostroumov et al., 2018). However, as mentioned earlier, the on-board interrogators can only interrogate a maximum of two beacons at any one time, limiting the accuracy (Vitan et al., 2015). Navigation by multiple DMEs is considered in pseudo ranging (Lo et al., 2020), however it requires modification of ground and on-board equipment.

If the aircraft were stationary (e.g., a hovering helicopter), it could sequentially interrogate different pairs of beacons, and thus progressively improve its position determination (Jalloul et al., 2014). Clearly this option is not applicable to most flying situations, where aircraft position is changing all the time. Instead, in Section 2 is prosed the way to create multiple simultaneous virtual distance measurements by using regression models to predict the aircraft's distance from beacons that are not being interrogated at a given moment.

2. Multiple distances in DME/DME

Our approach to distance measurement increases the number of available distance estimates by using the measurements to the current optimal DME pair as well as the extrapolated distances to previous optimal pairs. While conceptually simple, this approach requires three

computationally non-trivial steps: (1) selecting appropriate DME pairs, (2) extrapolating the previous distance measurements to estimate the current distances, and (3) since there are now multiple pairs of distances, solving navigation equation with multiple pairs of distances, rather than just one.

2.1. DME selection

The first problem to address is the selection of DME pairs to interrogate and subsequently extrapolate from. At the one extreme, the DME interrogator could rapidly and repeatedly cycle through all the available pairs, extrapolating between measurement instances. This approach reduces the duration of extrapolation needed for each measurement, but sacrifices the accuracy offered by the optimal pair. It would also require changes to the FMS software.

At the other extreme is the approach currently programmed into FMS, whereby the DME interrogator polls only the optimal pair and extrapolates distances from the previous optimal pairs. Figure 3 illustrates the polling process.

The aircraft FMS detects the optimal pair of DME/DME beacons that minimizes the position error and automatically tunes the on-board interrogators to the applicable frequencies. DME A and DME B are the optimal pair for the first part of the aircraft's trajectory. This pair is optimal for the first three sets of measurements (DA_1, DB_1, DA_2, DB_2, DA_3, DB_3). As the aircraft moves away from these DMEs, they are no longer optimal; instead DME C and DME D are now the optimal pair, from which the aircraft obtains the next two measurements (DC_1, DD_1).

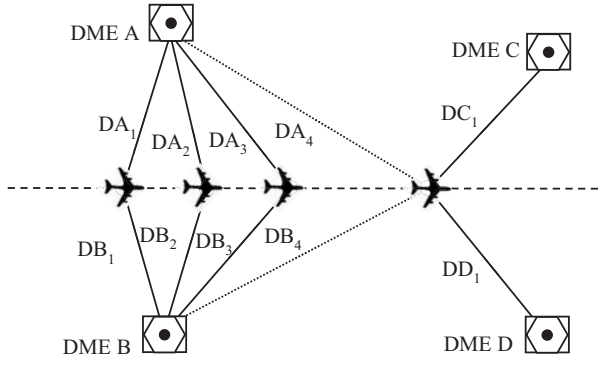

Figure 3. Multiple DME/DMEs approach

Once each pair is no longer optimal, its measurements were extrapolated.

The overall measurement accuracy increases as the number of (accurate) distance measurements increases, but the extrapolation error on these measurements also increases as time goes on. Therefore, there is some optimal number of DME pairs from which to extrapolate. This optimal number depends on both the extrapolation method and the relative dynamics of the aircraft and DME beacons (which in turn also affect the choice of extrapolation method).

2.2. Extrapolation of DME data

The next step is to extrapolate distances from the selected previous optimal pair measurements. The rate at which the distance to a DME beacon changes is determined by the aircraft's speed and position, as shown in Figure 4. When the aircraft is directly overhead the DME, this rate is roughly equal to the aircraft's speed. When the aircraft is away from the DME, only part of its velocity is seen by the distance measurement, and therefore the rate varies with time, as the horizontal and vertical angles to the DME beacons vary. Therefore, simple sequential operations or linear Kalman filter are not appropriate to use for distance data extrapolation. Instead, a regression model is used.

Regression is widely used for data extrapolation. The essence of regression is to approximate some set of data by a function, minimizing some set of errors. Linear regression is the simplest and most widely used type of regression (Seber & Lee, 2012, p. 35). Polynomials, exponentials, logarithms, and other functions can also be used as regression functions. When the regression involves a series of connecting segments, it is referred to as a spline. A spline function is a piecewise smooth polynomial function, the first and second derivatives of which are continuous everywhere on the curve. A B-spline, or basis spline, is a generalization of the Bezier curve. B-splines are defined by their order m and number of interior knots n. The degree of the B-spline polynomial is $(m - 1)$. To construct a B-spline, it is necessary to select for each segment a set of control points that set the general shape of the curve. The number of points may vary from one segment to another, without changing the order of the polynomial.

To achieve the desired smoothness, the first step is to choose the order B-splines. Polynomials of lower orders give low flexibility in controlling the shape of the curve.

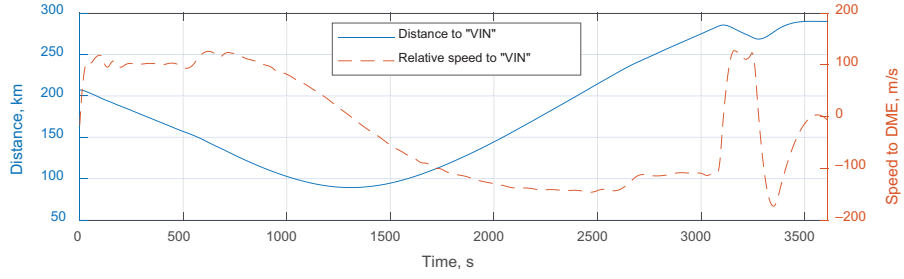

Figure 4. Distance from an aircraft to "VIN" DME during the flight "AUI79" and their mutual speed

First order B-splines are not sufficiently smooth in that they do not guarantee continuous derivatives. Second-order B-splines give a smoother curve, but may not be smoothly continuous at segment unions. Cubic B-splines that are C^0, C^1 and C^2 continuous are sufficiently smooth and also sufficiently smoothly continuous at segment unions. Higher order B-splines are more computationally intensive and can lead to undesirable approximation leaps. Therefore, cubic splines were selected.

The results of distance measurement D can be represented as follows:

$$D(t) = S(t) + \varepsilon, \tag{1}$$

where $S(t)$ are cubic splines with a second order continuity and ε is a random error vector.

The function $S(t)$ given and continuous on the segment $[a, b]$ is called a spline of m order with knots τ_i. The knot vector τ divides the interval [a, b] into a set of knot spans $(\tau_i, \tau_{i+1}]$. These subintervals enable us to create spline function at each segment.

The knots of the spline functions are arranged in increasing order such that $a \le \tau_0 < \tau_1 \ldots < \tau_n \le b$; $i = [1, n]$. The first knot of the spline functions coincides with the beginning of the observation data $\tau_0 = 0$, and the final knot corresponds to the last value of the observation time, $\tau_N = T$. Since the results of observations of a real process were dealt, the observations are ordered such that $t_1 = 0 < t_2 < \ldots < t_n = T$, and the penultimate knot τ_{N-1} occurs before the final observation $\tau_{N-1} < T$.

In the general case, B-splines can be written as:

$$S(t) = \sum_{j=1}^{N+3} B_{j,m}(t) P_j, \quad 0 \le t \le T, \tag{2}$$

where $S(t)$ is the result of the spline extrapolation at time t; P_j is a vector of spline function control points; and $B_{j,m}(t)$ are the basis functions of the B-spline.

The vector of control points contains two columns with time and corresponding values obtained from calculations based on the available measurement results. To obtain extrapolated values, it is necessary to evaluate the vector of control points and calculate the basis functions at the time of prediction.

The Cox-De Boor relation for the B-spline basis function (Yau et al., 2006; Siddiqi & Younis, 2013) was used. It defines the j^{th} basis function of B-spline of a specific order and has the form:

$$B_{j,1}(t) = \begin{cases} 1 \; if \; \tau_j \le t \le \tau_{j+1} \\ 0 \; if \; \tau_j > t > \tau_{j+1} \end{cases}$$

$$B_{j,m}(t) = \frac{t - \tau_j}{\tau_{j+m-1} - \tau_j} B_{j,m-1}(t) + \frac{\tau_{j+m} - t}{\tau_{j+m} - \tau_{j+1}} B_{j+1,m-1}(t), \tag{3}$$

where m is the order of B-spline.

The control points are calculated according to a known learning sample D that contains the results of the existing measurements and time measurements. Rewriting equation (2) in matrix form gives:

$$\boldsymbol{D} = \boldsymbol{BP}, \tag{4}$$

$$\boldsymbol{D} = \begin{bmatrix} d_1 & t_1 \\ d_2 & t_2 \\ \cdots & \cdots \\ d_n & t_n \end{bmatrix}; \; \boldsymbol{P} = \begin{bmatrix} p_1 & t_1 \\ p_2 & t_2 \\ \cdots & \cdots \\ p_n & t_n \end{bmatrix};$$

$$\boldsymbol{B} = \begin{bmatrix} B_{1,m}(t_1) & B_{2,m}(t_1) & B_{3,m}(t_1) & \cdots & B_{n,m}(t_1) \\ B_{1,m}(t_2) & B_{2,m}(t_2) & B_{3,m}(t_2) & \cdots & B_{n,m}(t_2) \\ \vdots & \vdots & \vdots & & \vdots \\ B_{1,m}(t_n) & B_{2,m}(t_n) & B_{3,m}(t_n) & \cdots & B_{n,m}(t_n) \end{bmatrix},$$

where P is the vector of control points and B is the matrix of basis functions calculated by Eq. (3).

Then, according to the known basis functions Eq. (3), the control points can be obtained from the solution of this equation (4) by the Least Squares Method:

$$\boldsymbol{P} = (B^T \boldsymbol{B})^{-1} B^T \boldsymbol{D}. \tag{5}$$

After obtaining matrix of control points Eq. (5) and basis functions from equation (3), equation (4) to extrapolate the distance at the required time (time of next measurement) was used.

Unbiased estimation of mean squared error of extrapolation can be obtained using the following expression (Seber & Lee, 2012, p. 44):

$$\sigma^2_{DMEp} = \frac{(\boldsymbol{D} - \boldsymbol{BP})^T (\boldsymbol{D} - \boldsymbol{BP})}{n - (N + 3)}. \tag{6}$$

The accuracy depends on the amount of available data. More measurements will result in greater prediction accuracy. For example, Figure 5 shows how the learning sample size affects the extrapolation error.

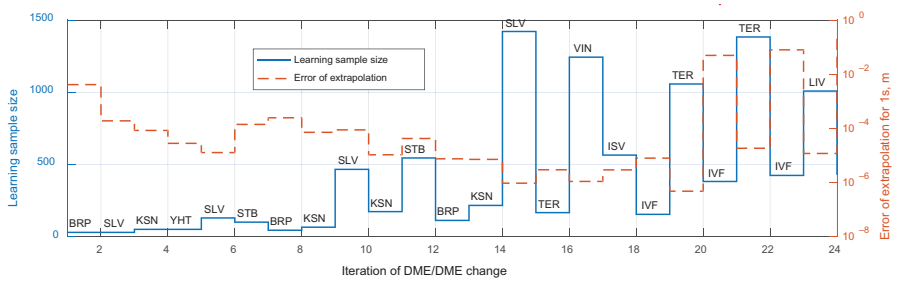

Figure 5. Learning sample size and extrapolation error value at each stage of distance prediction for flight "AUI79" (UKBB-UKLI) on June 1, 2018

2.3. Positioning by multiple DMEs

Obtained coordinates of aircraft location (x_{ACFT}, y_{ACFT}) in the horizontal plane of the local Cartesian coordinate system for multiple DME data by solving the following navigation equation:

$$d_{hi}^2 = \left(x_{ACFT} - x_{\mathrm{DMEi}}\right)^2 + \left(y_{ACFT} - y_{\mathrm{DMEi}}\right)^2, \quad (7)$$

where x_{DMEi}, y_{DMEi} are the coordinates of the i^{th} DME location and d_{hi} is the horizontal range between the i-th DME and the aircraft.

Equation (7) can be represented in matrix form for N DMEs as follows:

$$D^2 = \left(x_{\mathrm{ACFT}} - X_{\mathrm{DME}}\right)^2 + \left(y_{\mathrm{ACFT}} - Y_{\mathrm{DME}}\right)^2, \quad (8)$$

where $D = [d_{h1}, d_{h2}, ..., d_{hN}]$; $X_{DME} = [x_{DME1}, x_{DME2}, ..., x_{DMEN}]$; $Y_{DME} = [y_{DME1}, y_{DME2}, ..., y_{DMEN}]$.

Solved the system of nonlinear equations in Formula (8) using an iterative approach with linearization of equations with the help of a Taylor series expansion (Tian et al., 2013), beginning with the initial aircraft location (x_0, y_0). With each iteration the aircraft location becomes more precise, until the required accuracy of the solution is achieved. Equation (7) can be represented as a function of unknown variables (x_{ACFT}, y_{ACFT}):

$$d\left(x_{\mathrm{ACFT}}, y_{\mathrm{ACFT}}\right) = \sqrt{\left(x_{\mathrm{ACFT}} - x_{\mathrm{DME}}\right)^2 + \left(y_{\mathrm{ACFT}} - y_{\mathrm{DME}}\right)^2}. \quad (9)$$

Then, a first-order Taylor expansion gives a linear dependence for unknown variables Δx, Δy:

$$D\left(x_{\mathrm{ACFT}} + \Delta x, y_{\mathrm{ACFT}} + \Delta y\right) \approx D\left(x_{\mathrm{ACFT}}, y_{\mathrm{ACFT}},\right) + \frac{\partial D}{\partial x_{\mathrm{ACFT}}}\Delta x + \frac{\partial D}{\partial y_{\mathrm{ACFT}}}\Delta y. \quad (10)$$

Δx and Δy represent the difference in coordinates between initial searching point (x_0, y_0) and true aircraft location (x_{ACFT}, y_{ACFT}):

$$x_0 = x_{ACFT} + \Delta x;\ y_0 = y_{ACFT} + \Delta y. \quad (11)$$

Equation (10) has only approximate equality because only the first order of derivatives was used. Next iteration was improving the solution. Firstly, the equation of Formula (10) is represented in this form:

$$d\left(x_0, y_0\right) \approx d\left(x_{\mathrm{ACFT}}, y_{\mathrm{ACFT}}\right) + \frac{\partial d}{\partial x_{\mathrm{ACFT}}}\Delta x + \frac{\partial d}{\partial y_{\mathrm{ACFT}}}\Delta y. \quad (12)$$

Equation (8) can be represented in form of distances (D_0) to initial searching point of aircraft location (x_0, y_0):

$$D_0^2 = \left(x_0 - x_{\mathrm{DME}}\right)^2 + \left(y_0 - y_{\mathrm{DME}}\right)^2. \quad (13)$$

Partial derivatives of (13) by coordinates are:

$$\frac{\partial d}{\partial x_{\mathrm{ACFT}}} = \frac{x_0 - X_{DME}}{D_0};\ \frac{\partial d}{\partial y_{\mathrm{ACFT}}} = \frac{y_0 - Y_{DME}}{D_0}. \quad (14)$$

Substituting the resulting partial variables into equation (12):

$$d\left(x_0, y_0\right) \approx d\left(x_{\mathrm{ACFT}}, y_{\mathrm{ACFT}}\right) + \frac{x_0 - X_{DME}}{D_0}\Delta x + \frac{y_0 - Y_{DME}}{D_0}\Delta y. \quad (15)$$

It was denoted:

$$\Delta d = \frac{x_0 - X_{DME}}{D_0}\Delta x + \frac{y_0 - Y_{DME}}{D_0}\Delta y. \quad (16)$$

Rewriting in matrix form gives:

$$\Delta \boldsymbol{D} = \boldsymbol{H}\Delta \boldsymbol{X}, \quad (17)$$

where

$$\boldsymbol{H} = \begin{bmatrix} \frac{x_0 - x_{DME1}}{D_{01}} & \frac{y_0 - y_{DME1}}{D_{01}} \\ \frac{x_0 - x_{DME2}}{D_{02}} & \frac{y_0 - y_{DME2}}{D_{02}} \\ \cdots & \cdots \\ \frac{x_0 - x_{DMEN}}{D_{0N}} & \frac{y_0 - y_{DMEN}}{D_{0N}} \end{bmatrix};\quad \Delta \boldsymbol{X} = \begin{bmatrix} \Delta x \\ \Delta y \end{bmatrix};$$

$$\Delta \boldsymbol{D} = \begin{bmatrix} D\text{-} - D \\ D\text{-} - D \\ \cdots \\ D_{0N} - D_N \end{bmatrix}.$$

The unknown matrix ΔX can be calculated from Eq. (17) using the Least Squares Method in matrix form:

$$\Delta \boldsymbol{X} = (\boldsymbol{H}^T\boldsymbol{H}^{-1})^T\boldsymbol{H}^T\Delta \boldsymbol{D}. \quad (18)$$

Values of $\Delta \boldsymbol{X}$ are used as input information for defining the initial search points in subsequent iterations:

$$X_{i+1} = X_i - \Delta \boldsymbol{X}. \quad (19)$$

The computation can be continued until the desired accuracy (ξ) is achieved:

$$\Delta x^2 + \Delta y^2 \le \xi^2. \quad (20)$$

This approach rapidly improves precision. For example, Figure 6 shows the error as function of iteration for the 3613 different positioning calculations associated with the AUI79 flight trajectory. The error reduces to 10^{-10} m by the fourth iteration for the majority of calculations (99.94%).

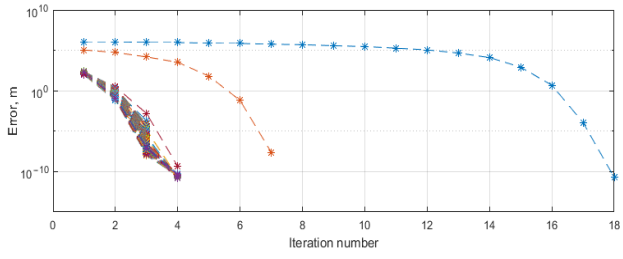

Figure 6. The error decreases rapidly as the number of iterations increases

3. Performance analysis

In this section, firstly, the equations for positioning accuracy estimation were used, and then the algorithm's performance was assessed using actual flight data.

3.1. Error measurement

Suggested algorithm performance in terms of accuracy and availability was considered. The mean-squared deviation error of positioning was characterised. Positioning availability, as defined by ICAO, is the percentage of time during which the desired accuracy can be guaranteed (International Civil Aviation Organization, 2017).

Derived the error term by expanding equations of Formula (9) using a first-order Taylor series, taking into account a random measurement error (ε):

$$f(D+\Delta D)\approx f(D)+\frac{df(D)}{dx}\Delta x+\frac{df(D)}{dy}\Delta y+\varepsilon, \quad (21)$$

where $f(D + \Delta D)$ is a function of distance measurements; $f(D)$ is a function of the true distances; and Δx, Δy are the errors in the x and y directions respectively.

The error in the distance determination is:

$$\Delta D=\frac{df(D)}{dx}\Delta x+\frac{df(D)}{dy}\Delta y+\varepsilon. \quad (22)$$

In matrix form, Equation (21) becomes:

$$\Delta D = \boldsymbol{H}^{T}_{DME}\,\boldsymbol{W}^{-1}\Delta, \quad (23)$$

where $W^{-1} = \mathrm{E}\{\varepsilon\,\varepsilon^{\mathrm{T}}\}^{-1}$ is the inverse correlation matrix of measurement equipment errors, or weight matrix; $\Delta^{T} = [\Delta x\ \Delta y]$ is matrix of errors in the direction of the axes; and H_{DME} is a matrix of partial derivatives:

$$\boldsymbol{H}_{DME}=\begin{bmatrix}\frac{df(D_1)}{dx} & \frac{df(D_1)}{dy}\\ \frac{df(D_2)}{dx} & \frac{df(D_2)}{dy}\\ \cdots & \cdots\\ \frac{df(D_N)}{dx} & \frac{df(D_N)}{dy}\end{bmatrix}.$$

The weight matrix W accumulates the mean square errors of distance detection and will be used for estimation of positioning error in horizontal plane by Weighted Least Squares Method:

$$\boldsymbol{W} = diag(S), \quad (24)$$

$$\boldsymbol{S}=\left[\bar{\sigma}_{DME1},\sigma_{DME2},\ldots,\sigma_{DMEN}\right].$$

The total matrix of distance detection errors (S) is the sum of distance measurement by equipment error (S_m) and prediction error (S_p):

$$\boldsymbol{S} = S_m + S_p, \quad (25)$$

where $S_m=\left[\bar{\sigma}_{DMEm1},\sigma_{DMEm2},\ldots,\sigma_{DMEmN}\right]$;

$S_p=\left[\bar{\sigma}_{DMEp1},\sigma_{DMEp2},\ldots,\sigma_{DMEpN}\right]$.

The weight matrix allows us to estimate the total accuracy of positioning taking into account the known prediction error. Since in the general case, both measured (S_m) and predicted (S_p) values are used in the system of navigation equations, the corresponding elements will be zero for the measured values. The elements of S_p matrix are estimated by Eq. (6) only for predicted distances. In case of measurements without prediction, the corresponding elements of S_p were set to zero.

The values $\sigma^{2}_{\mathrm{DMEm}}$ can be estimated as a sum of the error introduced by radio wave propagation in space $\sigma^{2}_{\mathrm{sis}}$ and the error introduced by the airborne interrogator σ^{2}_{air} (International Civil Aviation Organization, 2013):

$$\bar{\sigma}_{DMEm}=\sigma_{sis}+\sigma_{air}. \quad (26)$$

The space propagation error may not exceed 0.05 NM (International Civil Aviation Organization, 2013). The maximum error introduced by measurements of the airborne interrogator is given by (International Civil Aviation Organization, 2013):

$$\sigma^{2}_{air} = max\{0.085\ NM;\ 0.125\%R\},$$

where R is the measured distance to the DME.

To calculate H_{DME} the partial derivatives of equation (9) were taken:

$$\frac{df(D_i)}{dx}=\frac{x_{ACFT}-x_{\mathrm{DMEi}}}{D_i};\ \frac{df(D_i)}{dy}=\frac{y_{ACFT}-y_{\mathrm{DMEi}}}{D_i},$$

$$i = 1, n. \quad (27)$$

In case of multiple DMEs, the matrix of partial derivatives will have N rows corresponding to the number of DMEs and two columns corresponding to the coordinates of the airplane:

$$\boldsymbol{H}_{DME}=\begin{bmatrix}\frac{x_{ACFT}-x_{\mathrm{DME1}}}{D_1} & \frac{y_{ACFT}-y_{\mathrm{DME1}}}{D_1}\\ \frac{x_{ACFT}-x_{\mathrm{DME2}}}{D_2} & \frac{y_{ACFT}-y_{\mathrm{DME2}}}{D_2}\\ \cdots & \cdots\\ \frac{x_{ACFT}-x_{\mathrm{DMEN}}}{D_N} & \frac{y_{ACFT}-y_{\mathrm{DMEN}}}{D_N}\end{bmatrix}. \quad (28)$$

An error of coordinates determination can be written from Eq. (23) by Weighted Least Squares Method in matrix form:

$$\Delta = ((\boldsymbol{H}^{T}_{DME}\,\boldsymbol{W}^{-1}\boldsymbol{H}_{DME})^{-1}\,\boldsymbol{H}^{T}_{DME}\,\boldsymbol{W}^{-1})\Delta\boldsymbol{D}. \quad (29)$$

This expression indicates the dependence of the error of the coordinate determination on errors of the distance determination to DME. The matrix $(((H^{T}_{DME}\,W^{-1}H_{DME})^{-1}H^{T}_{DME})$ is called the least squares resolution matrix, and the matrix $((H^{T}_{DME}\,W^{-1}H_{DME})^{-1}\,H^{T}_{DME}\,W^{-1})$ is the solution matrix by the weighted Least Squares Method. It was considered that the error of DME measurement has Gaussian distribution with zero mean. Then the positioning accuracy can be represented as a covariance matrix of errors by coordinates:

$$cov(\Delta) = E[\Delta\,\Delta^{T}], \quad (30)$$

where E is the mathematical expectation.

Substituting Eq. (29) in Eq. (30):

$$cov(\Delta) = E[((H^T_{DME}\, W^{-1} H_{DME})^{-1}\, H^T_{DME}\, W^{-1})\Delta D\ (((H^T_{DME}\, W^{-1} H_{DME})^{-1}\, H^T_{DME}\, W^{-1})\Delta D)^T] =$$
$$E[(H^T_{DME}\, W^{-1} H_{DME})^{-1}\, H^T_{DME}\, W^{-1} \Delta D\ \Delta D^T H_{DME}\ (W^{-1})^T\ (H^T_{DME}\, W^{-1} H_{DME})^{-1}] =$$
$$(H^T_{DME}\, W^{-1} H_{DME})^{-1}\ (W^{-1})^T\ H^T_{DME} W^{-1}\ H_{DME}\ cov(\Delta D)\ (H^T_{DME}\, W^{-1} H_{DME})^{-1} =$$
$$(H^T_{DME}\, W^{-1} H_{DME})^{-1}\ (W^{-1})^T\ cov(\Delta D). \quad (31)$$

Since $(W^{-1})^T = W^{-1}$ and $cov(\Delta D) = W$:

$$cov(\Delta) = (H^T_{DME}\, W^{-1} H_{DME})^{-1}. \quad (32)$$

Thus, the mean-squared error of positioning in horizontal plane is:

$$\sigma^2_p = tr(H^T_{DME}\, W^{-1}\, H_{DME})^{-1}. \quad (33)$$

In case of positioning according to information from multiple DMEs, the location geometry of the navigational aids and aircraft has a significant influence on accuracy. The coefficient of dilution of precision (DOP) is determined by the geometry and variance σ_0. The DOP value in the horizontal plane (HDOP) is estimated using the navigation equation:

$$\overline{HDOP_{DME}} = \sigma_p \overline{\sigma_0}\ , \quad (34)$$

where σ_0 is the mean-squared error of the ground DME beacon.

Performance Based Navigation (PBN) is characterized by the Total System Error (TSE) value, which can be represented as the sum of the Flight Technical Error (FTE) and the Navigation System Error (NSE), which in turn includes the error of coordinate detection within a 95% confidence band:

$$TSE^2 = NSE^2 + FTE^2 = 4\sigma^2_p + FTE^2\,. \quad (35)$$

In the next section, the mean-squared error of positioning Eq. (33), HDOP coefficient Eq. (34), and TSE Eq. (35) to analyze the performance of our approach to positioning by multiple DME data.

3.2. Numerical application

This is an approach using a computer-based simulation with real flight data for the Ukrainian airspace. The accuracy of approach using multiple DMEs with the conventional pair-based approach was compared.

The flight data for flight AUI79 with an ERJ-135 aircraft from Boryspil (UKBB) to Ivano-Frankivsk (UKLI) on June 1, 2018 were used. Flight data is obtained from a network of SDRs which receive, decode, and collect reports of airplane location transmitted by 1090 ES onboard transponder under the Automatic Dependent Surveillance Broadcast (ADS-B). Flight data include latitude, longitude and barometrical altitude of airplane, which are measured onboard by GNSS sensor. The total flight time was 1 hour 28 minutes with actual distance 327 NM and cruise altitude 28,000 ft. Figure 7 shows the flight track along with the available DMEs for positioning.

The Standard Service Volume of DMEs (Federal Aviation Administration, 2020) to detect the available navigational aids at each aircraft location was used, and then the optimal DME/DME pair at that location, using the same algorithm used in FMS was selected. Figure 8 shows the navigation system error based on optimal pair selection together with the number of available pairs by time of flight.

The maximum acceptable prediction error to be equal to 370.4 m (Lilley & Erikson, 2012) was set. In other words, once the error from a particular DME prediction becomes greater than 370.4 m, we stop using that DME.

More than three DMEs are used for positioning 29% of the time (Figure 9). The result depends on the available navigational aids in the ground network and the optimal pair selection algorithm used inside of FMS. But, for a particular trajectory and set of equipment, it means that the proposed approach gives better positioning for about 29% of the total flight time.

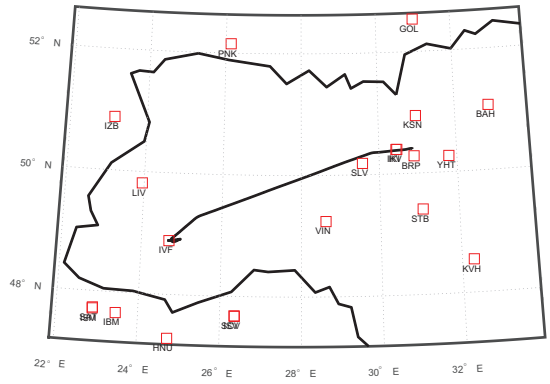

Figure 7. Flight track of "AUI79" in geodesic coordinate system with all available DMEs

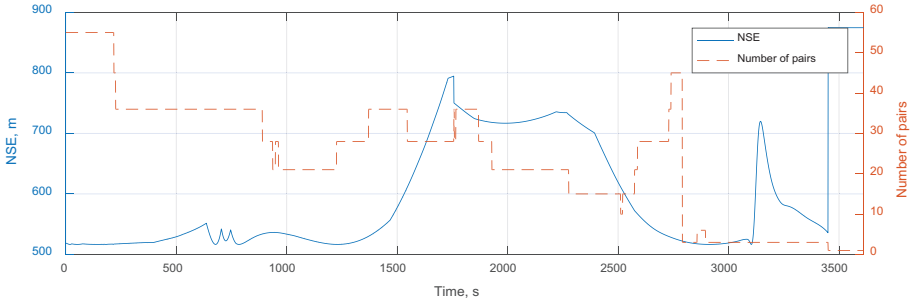

Figure 8. Navigation system error for optimal DME/DME pair and total number of pairs

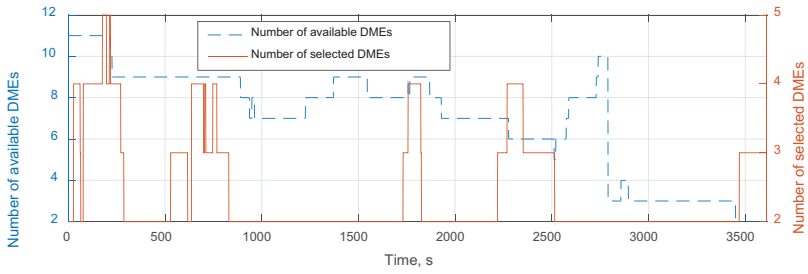

Figure 9. Number of DMEs in multi DME/DMEs approach

Figure 10 shows the results of mean-squared error of positioning in horizontal plane using equation (33) with prediction by regression model in comparison with prediction by Kalman approach and sequential operations. The dotted line indicates σ_p without considering errors of prediction, the solid blue line represents accuracy of positioning by optimal pair of DME/DME, and the solid black line indicates the result for the multi DMEs approach. When more than two DMEs are available (including predicted values), σ_p decreases. But, when the spline prediction error increases, σ_p increases too, degrading accuracy. Also, in Figure 10 the values of σ_p estimated with Kalman prediction and sequential operations are represented in comparison with prediction by regression model. The regression model extrapolation gives better accuracy in comparison with the Kalman approach and sequential operations. Decreasing of σ_p at time of positioning with predicted data results of HDOP and TSE values decreasing (Figures 11–12).

In our case the HDOP coefficient is a result of the errors of positioning, errors of measurements, and errors of prediction. The HDOP coefficient estimation (Figure 11), using multiple DME data extrapolated with a B-spline, indicates significant improvement in the geometrical factor in comparison with positioning only by one DME/DME pair. The geometry of the ground navigational aids and extrapolation errors cause large variation in HDOP over each flight. Our proposed approach helps to reduce the HDOP coefficient by as much as one, making the geometrical factor sufficient for navigation (Tahsin al., 2015).

The total system error (TSE) includes the $2\sigma_p$ confidence band for positioning error estimated by Eq. (35). We use FTE = 0.5 NM (Lo al., 2010) for the TSE calculation. Figure 12 shows that flight AUI79 can be supported with DME/DME positioning under RNAV 1 requirements.

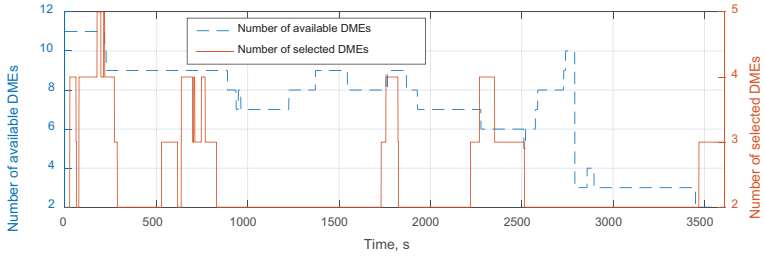

Figure 10. Mean-squared error of positioning in horizontal plane

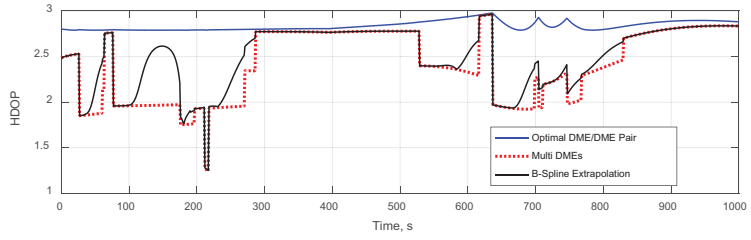

Figure 11. HDOP coefficient in case of B-spline extrapolation

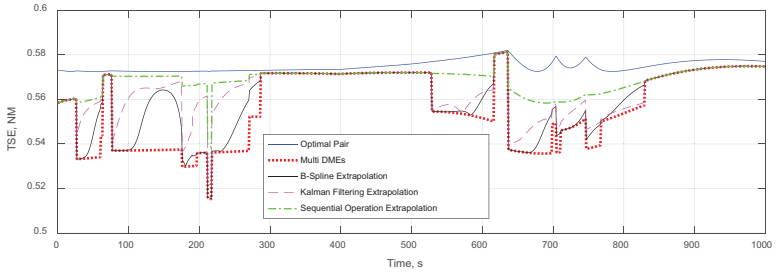

Figure 12. Total system error

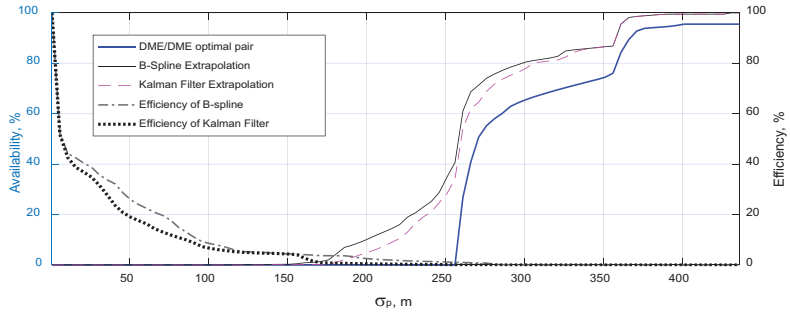

Figure 13. Availability of positioning by multiple DMEs

Figure 13 shows the availability (as a % of time) of positioning using multiple DMEs for equal σ_p values. The availability obtained with the B-spline extrapolation is consistently higher than availability estimation only by optimal DME/DME pair.

Increasing the number of DMEs used for positioning with the help of data extrapolation improves aircraft positioning accuracy. The linear regression model with B-Spline function performs better than the Kalman filer (Figure 13). Performance of positioning depends on the number of DMEs, their geometry, and the number of available measurements for extrapolation. Numerical demonstration for AUI79 flight data indicates efficiency of extrapolated data usage in comparison with only a pair of DME/DME measurements. Implementation of B-Spline for DME data extrapolation decreases σ_p at 50 m in 26% of flight time.

Conclusions

Results of presented analysis of primary positioning system malfunction indicate about 347 reported cases of GNSS failures in civil aviation for the last 15 years. Failures in primary positioning system reduce the safety of aviation significantly due to limited time of Inertial Reference Unit and low performance of positioning by DME/DME.

The proposed alternative positioning approach allows using measured and predicted by regression distances in DME/DME navigation. Accumulated distances to particular DME beacons are used for extrapolation by B-Spline functions. Predicted distances from efficient DMEs modify system of navigation equations and improve total positioning performance. This approach does not require modification of ground network of beacons and is compatible with the most of modern on-board FMS and DME interrogators. Also, its operation does not require interruption of the DME pair selection logic during positioning cycle in FMS. Thus, classical and proposed approaches can provide positioning simultaneously in FMS.

As an example, for trajectory of AUI79 flight, the proposed method gives better performance in comparison with DME/DME efficient pair algorithm in 29% of flight time. Moreover, a method gives improving of positioning performance in 50 m for σ_p in 26% of flight time.

Positioning accuracy depends on configuration of the ground beacons network and performance of on-board interrogators. The total system performance depends on relative airplane location and available ground network configuration. Therefore, reconfiguration and modernization of navigation aids network is one of the important tasks of each air navigation service provider in order to ensure the required level of flight safety.

References

Berz, G. (2008, April). *Guideline for P-RNAV infrastructure assessment*. Eurocontrol.

Federal Aviation Administration. (2017). *Federal NOTAM System*. Database Online. https://notams.aim.faa.gov

Federal Aviation Administration. (2020). *Aeronautical Information Manual*. Official Guide to Basic Flight Information and ATC Procedures, U.S. Department.

Han, S., Gong, Z., Meng, W., Li, C., & Gu, X. (2016). Future alternative positioning, navigation, and timing techniques: A survey. *IEEE Wireless Communications*, *23*(6), 154–160. https://doi.org/10.1109/MWC.2016.1500181RP

International Civil Aviation Organization. (2013). *Performance-Based Navigation (PBN) Manual (Doc 9613-AN/937)*. International Civil Aviation Organization. Montreal, Canada.

International Civil Aviation Organization. (2017). *Global Navigation Satellite System (GNSS) Manual (Doc. 9849)* (3 ed.). International Civil Aviation Organization. Montreal, Canada.

International Civil Aviation Organization. (2020). *Procedures for Air Navigation Services (PANS) – Aircraft Operations – Volume II, Construction of Visual & Instrument Flight Procedures (Doc 8168)* (7 ed.). International Civil Aviation Organization. Montreal, Canada.

Jalloul, T., Ajib, W., Yeste-Ojeda, O. A., Landry, R., & Thibeault, C. (2014, October). DME/DME navigation using a single low-cost SDR and sequential operation. In *2014 IEEE/AIAA 33rd Digital Avionics Systems Conference (DASC)* (pp. 3C2-1-3C2-93C2-1). IEEE. https://doi.org/10.1109/DASC.2014.6979451

Kim, H., Lee, J., Oh, S. H., So, H., & Hwang, D. H. (2019). Multi-radio integrated navigation system M&S software design for GNSS backup under navigation warfare. *Electronics, 8*(2), 188. https://doi.org/10.3390/electronics8020188

Kuzmenko, N. S., Ostroumov, I. V., & Marais, K. (2018, October). An accuracy and availability estimation of aircraft positioning by navigational aids. In *2018 IEEE 5th International Conference on Methods and Systems of Navigation and Motion Control (MSNMC)* (pp. 36–40). IEEE. https://doi.org/10.1109/MSNMC.2018.8576276

Lilley, R., & Erikson, R. (2012). *DME/DME for Alternate Position, Navigation, and Timing (APNT)*. APNT White Paper, August.

Lo, S., Chen, Y. H., Enge, P., Pelgrum, W., Li, K., Weida, G., & Soelter, A. (2020). Flight test of a pseudo-ranging signal compatible with existing distance measuring equipment (DME) ground stations. *NAVIGATION, Journal of the Institute of Navigation*, *67*(3), 567–582. https://doi.org/10.1002/navi.376

Lo, S., Chen, Y. H., Enge, P., Peterson, B., Erikson, R., & Lilley, R. (2013, September). Distance measuring equipment accuracy performance today and for future alternative position navigation and timing (APNT). In *Proceedings of the 26th International Technical Meeting of The Satellite Division of the Institute of Navigation (ION GNSS 2013)* (pp. 711–721). Nashville, TN.

Lo, S., Enge, P., Niles, F., Loh, R., Eldredge, L., & Narins, M. (2010). Preliminary assessment of alternative navigation means for civil aviation. In *Proceedings of the 2010 International Technical Meeting of The Institute of Navigation, CA ION ITM* (pp. 314–322). San Diego.

Lubbers, B., Mildner, S., Oonincx, P., & Scheele, A. (2015, October). A study on the accuracy of GPS positioning during jamming. In *Navigation World Congress (IAIN)* (pp. 1–6). 2015 International Association of Institutes. IEEE. https://doi.org/10.1109/IAIN.2015.7352258

NASA. (2020). *Aviation Safety Reporting System*. Database Online. https://asrs.arc.nasa.gov/search/database.html

Ostroumov, I. V., & Kuzmenko, N. S. (2018, October). An area navigation RNAV system performance monitoring and alerting. In *2018 IEEE First International Conference on System Analysis & Intelligent Computing (SAIC)* (pp. 211–214). Kyiv, Ukraine. https://doi.org/10.1109/SAIC.2018.8516750

Ostroumov, I. V., Kuzmenko, N. S., & Marais, K. (2018, October). Optimal pair of navigational aids selection. In *2018 IEEE 5th International Conference on Methods and Systems of Navigation and Motion Controlm (MSNMC)* (pp. 32–35). IEEE. https://doi.org/10.1109/MSNMC.2018.8576293

Ostroumov, I., Kharchenko V., & Kuzmenko, N. (2019). An airspace analysis according to area navigation requirements. *Aviation*, *23*(3), 36–42. https://doi.org/10.3846/aviation.2019.10302

Seber, G. A., & Lee, A. J. (2012). *Linear regression analysis* (Vol. 936). John Wiley & Sons.

Siddiqi, S. S., & Younis, M. (2013). Construction of m-point binary approximating subdivision schemes. *Applied Mathematics Letters, 26*(3), 337–343. https://doi.org/10.1016/j.aml.2012.09.016

Tahsin, M., Sultana, S., Reza, T., & Hossam-E-Haider, M. (2015, May). Analysis of DOP and its preciseness in GNSS position estimation. In *2015 International Conference on Electrical Engineering and Information Communication Technology (ICEEICT)* (pp. 1–6). IEEE. https://doi.org/10.1109/ICEEICT.2015.7307445

Tian, A., Dong, D., Ning, D., & Fu, C. (2013, October). GPS single point positioning algorithm based on least squares. In *2013 Sixth International Symposium on Computational Intelligence and Design* (Vol. 2, pp. 16–19). IEEE. https://doi.org/10.1109/ISCID.2013.119

Vitan, V., Berz, G., & Solomina, N. (2015, September). Assessment of current DME performance and the potential to support a future A-PNT solution. In *2015 IEEE/AIAA 34th Digital Avionics Systems Conference (DASC)* (pp. 2A2-1-2A2-182A2-1). IEEE. https://doi.org/10.1109/DASC.2015.7311357

Yau, H. T., Lin, M. T., & Tsai, M. S. (2006). Real-time NURBS interpolation using FPGA for high speed motion control. *Computer-Aided Design, 38*(10), 1123–1133. https://doi.org/10.1016/j.cad.2006.06.005

Notations

Variables and functions

$B_{j,m}(t)$ – basis functions of the B-spline;
d_{hi} – horizontal range between the i-th DME and the aircraft;
$\boldsymbol{H}_{\text{DME}}$ – matrix of partial derivatives;
m – Spline function order;
n – number of interior knots;
P_j – vector of control points;
R – measured distance to the DME;
$\mathbf{S}$ – matrix of distance detection errors;
$S(t)$ – cubic splines;
S_m – equipment error;
S_p – prediction error;
$\boldsymbol{W}$ – correlation matrix of measurement equipment errors;
x_0, y_0 – initial aircraft location;
x_{ACFT}, y_{ACFT} – are airplane coordinates in NED reference frame;
x_{DMEi}, y_{DMEi} – coordinates of the i^{th} DME location;
Δ – matrix of errors;
Δx and Δy – difference in coordinates;
ε – random error vector;
ξ – positioning accuracy;
σ_0 – mean-squared error of the ground DME beacon;
σ^2_{air} – error introduced by the airborne interrogator;
σ^2_{DMEp} – mean squared error of extrapolation;
σ^2_{p} – mean-squared error of positioning in horizontal plane;
σ^2_{sis} – error introduced by radio wave propagation in space;
τ_i – i^{th} knot;

Abbreviations

ADS-B – Automatic Dependent Surveillance Broadcast;
APNT – Alternative Positioning Navigation and Timing;
DME – Distance Measuring Equipment;
DOP – Dilution of Precision;
FMS – Fight Management System;
FTE – Flight Technical Error;
GNSS – Global Navigation Satellite Systems;
GPS – Global Positioning System;
HDOP – Horizontal Dilution of Precision;
LLA – Latitude, Longitude and Altitude;
NED – Local Cartesian coordinate system North, East, Down;
NDB – Non-Directional Beacon;
NSE – Navigation System Error;
PBN – Performance Based Navigation;
RNAV – Area Navigation;
TACAN – Tactical Air Navigation;
TSE – Total System Error;
VOR – Very High Frequency Omnidirectional Range;
UHF – Ultra High Frequency.